Materials Today: Proceedings xxx (xxxx) xxx

Contents lists available at ScienceDirect

Materials Today: Proceedings

journal homepage: www.elsevier.com/locate/matpr

Antibacterial effect of silver nanoparticles synthesised on a polycarbonate membrane

J. Sackey [a,b,*], A. Fell [a,b], J.B. Ngilirabanga [c], L.C. Razanamahandry [a,b], S.K.O. Ntwampe [d,e], M. Nkosi [a,b]

[a] Nanosciences African Network (NANOAFNET), iThemba LABS-National Research Foundation, Old Faure Road, 7129 Somerset West, South Africa
[b] UNESCO-UNISA Africa Chair in Nanosciences/Nanotechnology, College of Graduate Studies, University of South Africa (UNISA), Muckleneukridge, P.O. Box 392, Pretoria, South Africa
[c] University of Western Cape, School of Pharmacy, Robert Sobukwe Rd, Bellville, Cape Town 7535, South Africa
[d] Department of Chemical Engineering, Faculty of Engineering and the Built Environment, P.O. Box 1906, Bellville, Cape Town 7535, South Africa
[e] Bioresource Engineering Research Group (BioERG), Faculty of Applied Sciences, P.O. Box 652, Cape Town 8000, South Africa

ARTICLE INFO

Article history:
Received 19 September 2019
Received in revised form 24 March 2020
Accepted 8 April 2020
Available online xxxx

Keywords:
Polycarbonate membrane
Silver nanoparticles
Green process
Callistemon viminalis
Anti-bacterial effect

ABSTRACT

This work reports for the first time the possibility of green synthesis and the antibacterial effect of silver nanoparticles (AgNPs) on commercialized polycarbonate membrane. The AgNPs were loaded on the polycarbonate membrane serving as the substrate via ultra-sonication and centrifugation. The extracts from the red flowers of *Callistemon viminalis* were used as the chelating agent. The synthesised thin film silver nanoparticles were characterized by various techniques such as Scanning Electron Microscope (SEM), Energy Dispersive X-ray spectroscopy (EDX), Fourier transform-infrared (FT-IR), X-Ray diffraction and UV–Vis spectroscopy. Consequently, the antibacterial affect was studied. The synthesised thin film silver nanoparticles had a surface plasmon resonance of 310nmand show a very effective inhibition growth of both Gram-positive and Gram-negative.

Selection and peer-review under responsibility of the scientific committee of the NANOSMATAFRICA-2018.

1. Introduction

Silver nanoparticles (AgNPs) are among the noble metals studied extensively due to their unique physical and chemical properties. They have found application in areas such as water and air purifiers, imaging, textiles, sensors, energy sector, antibacterial products and anticancer agents [1–4]. AgNPs have strong optical absorption which is attributed to intra-band quantum excitations of the conduction electrons making them good candidates for technological applications, for instance in surface enhanced resonance Raman scattering [5] optical biosensor and photo-catalysis. AgNPs can be synthesized by either chemical or physical approach such as evaporation, sputtering, e-beam, pulsed laser ablation, spark processing, glow discharge growth, rapid oxidation of metal tin, microwave mediated synthesis, hydrothermal, solvothermal, colloidal growth, solegel, chemical vapor deposition, spray pyrolysis, sonochemistry, hydrolysis, self-assembly, electrodeposition, electrospinning and carbothermal reduction processes among others [6–13].

Most of these methods though efficient in achieving nanoparticles of desired sizes and shapes, are difficult to attain pure particles, have complicated preparation procedures and even produce toxic by-products that may harm the environment. Recently, in addition to the physical and chemical methodologies, green processes using natural extracts as chelating agents have been demonstrated to be very effective in the synthesis of a variety of nanoscaled oxides including silver oxides. The green process eliminate the use of toxic materials, is clean, reliable, biocompatible, benign and eco-friendly.

The idea of synthesising nanoparticles on permeable substrate – filter paper or aluminum based membranes has been approached previously from different perspectives by several research groups. Specially, for the silver nanoparticles, the substrate preparation has been based either on the filtration of silver colloids through polymeric membranes [14] or on the chemical reduction of silver directly on the filter surface [15]. Other methods [16] of assembling arrays of silver nanoparticles on the surface of track etch polycarbonate membranes have been investigated. Hassan et al. [17] loaded silver nanoparticles on MMA/HEMA copolymer to show the effectiveness of nanoparticles in supporting paper

* Corresponding author at: Nanosciences African Network (NANOAFNET), iThemba LABS-National Research Foundation, Old Faure Road, 7129 Somerset West, South Africa.
E-mail address: sackey@tlabs.ac.za (J. Sackey).

https://doi.org/10.1016/j.matpr.2020.04.121
2214-7853/
Selection and peer-review under responsibility of the scientific committee of the NANOSMATAFRICA-2018.

properties. Manimegalai et al. [18] used cellulose acetate membrane (CAM) as support for silver nanoparticles (AgNPs) in the mineralization of pesticides in water. Wang et al. [19] loaded silver nanoparticles on a highly porous cellulose acetate nanofibrous membrane for treatment of dye wastewater. Zhang et al. [20] used PVA as a reducing and stabilizing agent to immobilize AgNPs on commercial NF membrane surface for anti-biofouling. Manimegalai et al. [21] synthesized AgNPs supported on cellulose acetate membrane to estimate it mineralization potential.

This contribution reports a cost effective but efficient green synthesis of thin film silver nanoparticles on a polycarbonate membrane via ultra-sonication and centrifugation for anti-bacterial studies.

1.1. Biosynthesis processes and materials

Callistemon viminalis also known as weeping bottlebrush is a shrub or small tree of the Myrtaceae family native to Australia. The plant has been reported to have various medicinal values such as antibacterial, antifungal, antioxidant activities and other pharmaceutical and insecticidal properties. It has bright red flower spike which occurs between spring and summer. The red dye extracts obtained from *Callistemon* red flowers, are rich in flavonoids, saponins, steroids, alkaloids and triterpenoids [22]. It was evident from the literature that amino acid is considered as effective reducing agent Therefore mechanism of formation of AgNPs using aqueous extracts from *Callistemon viminalis* is proposed based on the chemical reaction of the amino acid with the precursor salt.

This study report the synthesis of single phase AgNPs using the red dye extracts of the *Callistemon viminalis* via the green process on a polycarbonate membrane as substrate. Briefly, the procedure is as follows; fresh red flowers of *Callistemon viminalis* collected from iThemba LABS were dried under the sunlight. 5.6 g of the flowers were boiled in 66.6 mL of deionized water for 2 hrs and filtrated twice upon cooling to remove any residue. 1.5 g of silver nitrate precursor purchase from Sigma–Aldrich was dissolved in 20 mL of the obtained extracts. A black colour solution began to precipitate within 10 min.

Two approaches were used for loading the silver nanoparticles on the substrate (polycarbonate membrane). The protocol is as follows; a 3 × 3 cm commercialized polycarbonate membrane of pore size 50 nm was used. Firstly, one membrane (labelled as S1) was placed inside the black solution and centrifuged at 4000 rpm. And secondly, another membrane (labelled as S2) was ultrasonicated for 24 hrs. The thin film samples were later dried in air and characterized by the various techniques.

1.2. Antibacterial test

The antibacterial effect of the three thin film samples (S1, S2 and V) was studied by testing two types of microorganisms: *Escherichia coli* and *Bacillus cereus* which are gram negative and gram positive bacteria, respectively. Samples S1 and S2 are formed by silver nanoparticles loaded on a polycarbonate membrane as a substrate. Sample V is the polycarbonate membrane without silver nanoparticle, and it serving as the control. A medium enriched by Agar nutrient purchased at Sigma Aldrich in South Africa was prepared. A mass of 15 g of the Agar nutrient was added into 1 L of deionised water and sterilised in the autoclave for 15 min at 121 °C. The sterilised agar solution was distributed into petri dishes with a volume of 12 ml per petri dish and let to solidify at room temperature. Then, microorganisms were streaked on the solidified agar nutrient. Each petri dish was divided in three parts marked by a line. Each sample (S1, S2 and V) was stacked at the middle of each part. Then the petri dishes were incubated directly at 37 °C for 24 h. All steps of analysis were conducted under sterile conditions.

1.3. Characterization techniques

The phase identification of the synthesized thin film samples were analyzed by X-Ray diffraction using a Bruker AXS D8 advance with radiation ($\lambda_{Cuk\alpha}$ = 1.5406 Å). Fourier transform-infrared (FT-IR) absorption spectrometer (Shimadzu 8400 s spectrophotometer) was used to identify the functional groups. The samples were coated in EM1 Tech (K950X) deposition system with a thin gold palladium ultra-layer (25 Å), and imaged by Carl zeiss Auviga Scanning Electron Microscope (SEM) operated at 5 keV. The chemical compositions of the thin film samples were studied with Energy-Dispersive X-ray spectroscopy (EDS, Oxford instrument with X-max Solid state silicon drift detector at 20 keV. Thermogravimetric (TGA) analysis of the synthesized thin film samples was performed on Perkin Elmer (TGA 4000) with heat from 30.00 °C to 850.00 °C at 10.00 °C/min under nitrogen atmosphere. The samples were imaged on a Nikon SMZ 1500 optical microscope of C-W 10XB/22 Nikon lens with DS-F12 Nikon camera and an LED Ring light source. The analysis was done with the Nikon Imaging Software vision D (NIS-Elements F 4.00.00). The optical measurement was performed on Cary 5000 series UV–Vis-NIR spectrophotometer equipped with an integrating sphere.

2. Result and discussion

2.1. Sem, psd, eds

The distribution of silver nanoparticles on the surface polycarbonate membrane is illustrated by the SEM images in Fig. 1(a,b). The histogram of the particle distribution is shown in Fig. 1(c). The average particle size distribution (PSD) was estimated as 58.5 nm. Clearly, the nanoparticles are monodispersed on the surface of the substrate. The high monodispersion of the synthesized AgNPs could be attributed to the extracts which acts as reducing agent. The elemental analysis of the synthesis thin film samples is showed in (Fig. 1d). Silver was identified on the samples. Carbon originate from the carbon coated grid.

2.2. Chemical bonds/phase identification

ATR /FTIR spectroscopy indicates the chemical bonding/vibrations and frequency analysis of compounds at the atomic level. Fig. 2 report similar transmittance peaks for virgin and modified membranes. Besides the broad shoulder around 3397 cm^{-1}on S2, the peak at 2975 cm^{-1} can be assigned to C-H stretching vibration of the CH_3 groups while 1772 cm^{-1} can be attributed to the C=O stretching of the carboxylic anhydrides [23]. The Amide II band for N-H inplane bending appears at 1512 cm^{-1} [24]. The peaks at 1243 cm^{-1} are related to C–O group acetyl [25], other vibrations at 1022 cm^{-1} is due to C-N stretching of aliphatic primary amine [23].

The XRD spectra (Fig. 3) shows that S2 has a peak located at 2θ = 38° corresponding to reflection of the crystal plane with Miller indices (1 1 1). This is a characteristic peak of the Face-centered cubic silver with lattice parameter a = 4.08620 (JCPDS number 00-004-0783).

2.3. Optical analysis

Fig. 4 shows the optical analysis in terms of reflectance (a-b) and absorbance spectra (c-d). As can be observed, the reflectance on the virgin membrane (without AgNPs) (v) (see Fig. 4(a)) is

Please cite this article as: J. Sackey, A. Fell, J. B. Ngilirabanga et al., Antibacterial effect of silver nanoparticles synthesised on a polycarbonate membrane, Materials Today: Proceedings, https://doi.org/10.1016/j.matpr.2020.04.121

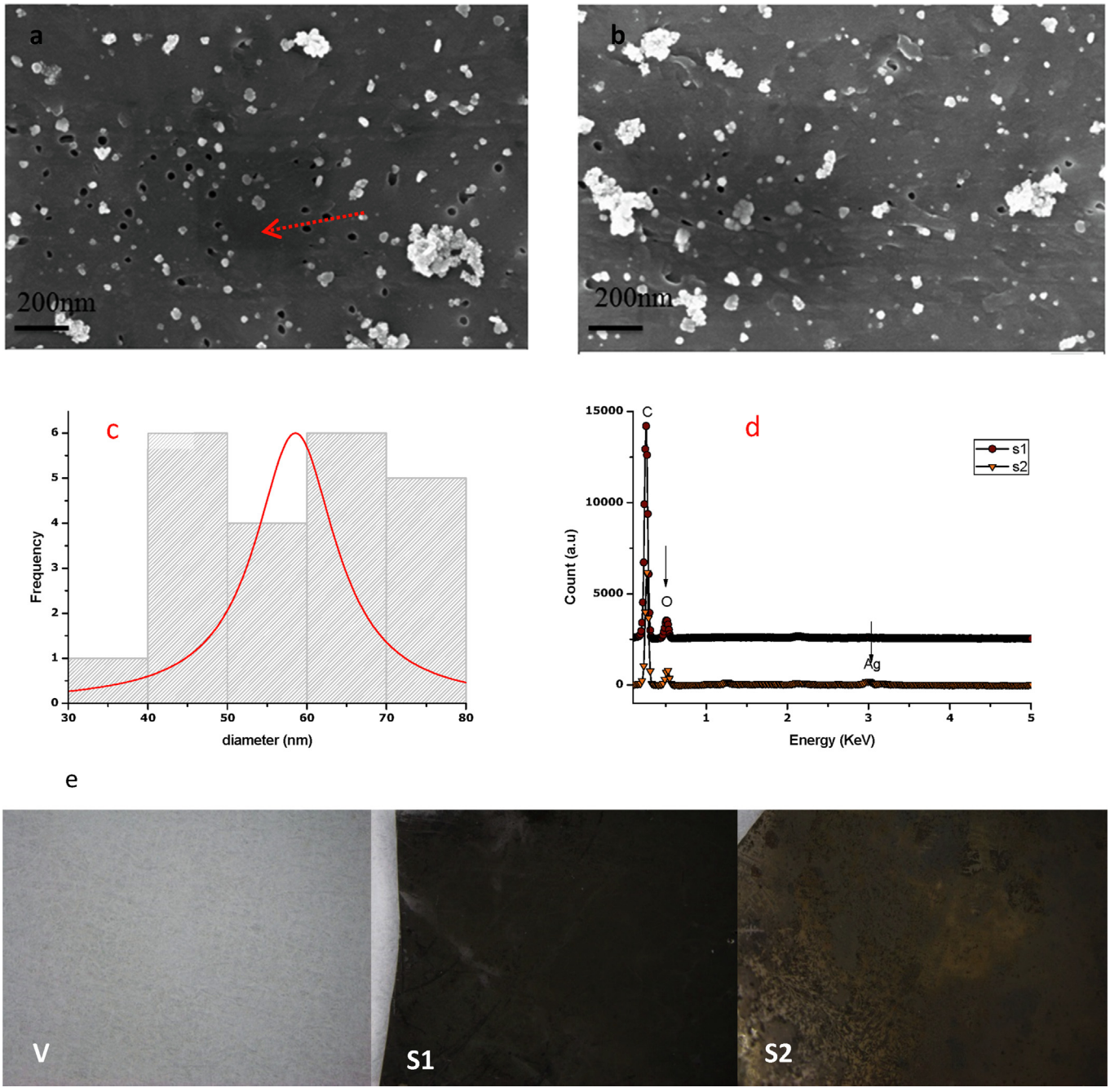

Fig. 1. (a,b) thin film synthesis of silver particles on the surface of (arrowed) polycarbonate membrane with pore size 0f 50 nm via (a) centrifugation, (b) ultra-sonication methods. Insect shows higher magnification of spherical-like nanoparticles, (c) the histogram of the particle size distribution with curve fitting provides an average size of 58.5 nm, (d) the EDS indicate chemical element of Ag, (e) optical images of the virgin membrane (v), and the thin film silver nanoparticles (S1 & S2).

higher than on the thin film AgNPs (S1& S2) in the visible wavelength region. In addition, interference fringes begin to appear in the IR region on all samples.

In the absorbance spectra (see Fig. 5), the AgNPs display strong Surface Plasmon Resonance (SPR) due to the coherent oscillations of conduction band electrons in resonance with the electromagnetic UV–visible light [26]. In particular, the AgNPs with particle size 58.5 nm exhibited steady absorbance peaks centered at 310 nm. Generally, the plasmon resonance of AgNPs is centered at 420 nm. The conduction energy band gap of the Ag nanoparticles was calculated indirectly from the absorption spectra via the Tauc's equation [27]:

$$(\alpha h\nu)^2 = A(h\nu - E_{gap}) \quad (1)$$

where α, $h\nu$ A, E_{gap} are linear absorption coefficient, Plank's constant, frequency of light, proportionality constant, Energy band gap respectively. This was achieved by plotting $(\alpha h\nu)^2$ vs $h\nu$ and extrapolating the curve down the energy axis. The results are reported in Fig. 6(a–c).

Fig. 7 represent the thermogravimetric analysis and its derivative form (TGA–DTG curves) on the modified membrane with the silver nanoparticles. The weight percentage is plotted as a function of temperature of the sample during heating from 30.00 °C to 850.00 °C at 10.00 °C/min. As can be observed, at a temperature

Please cite this article as: J. Sackey, A. Fell, J. B. Ngilirabanga et al., Antibacterial effect of silver nanoparticles synthesised on a polycarbonate membrane, Materials Today: Proceedings, https://doi.org/10.1016/j.matpr.2020.04.121

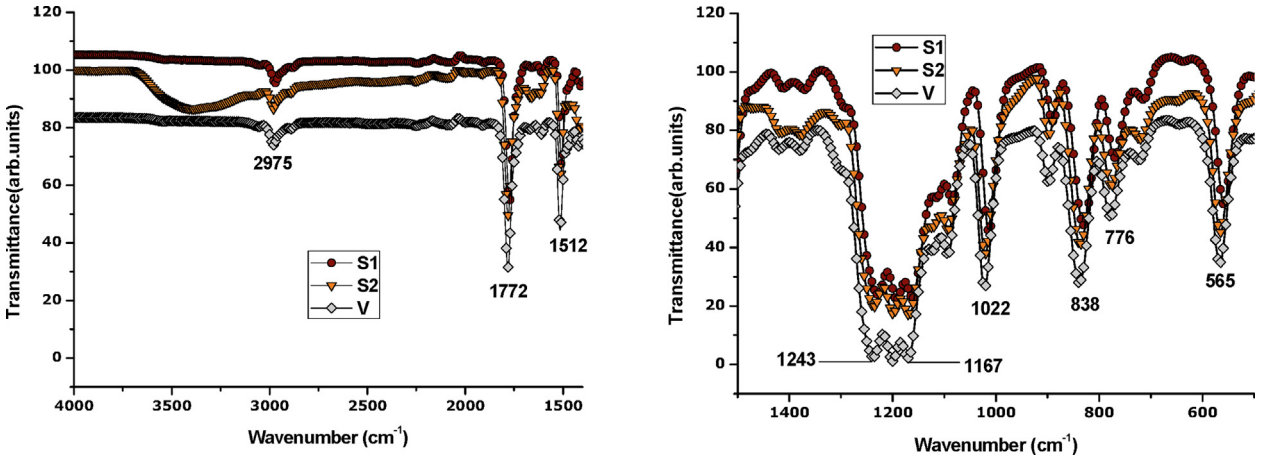

Fig. 2. The ATR spectra for the virgin polycarbonate membrane (V) and the silver nanoparticles (S1, S2).

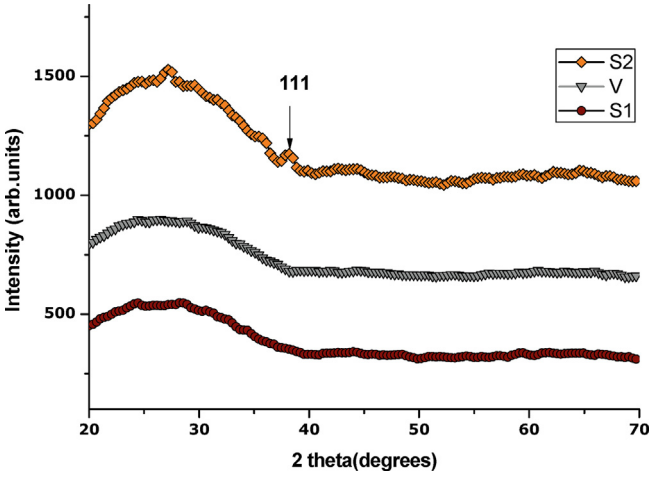

Fig. 3. The XRD spectra showing the virgin (V) polycarbonate membrane and (S1 & S2) modified membrane with silver nitrate.

from 100 °C, to 250 °C, the bottle brush begins to decompose slowly with a weight loss of 0.03%. At temperature of 375 °C, the capping agent continues to decompose with the main reduction of the sample occurring at 436 °C.

2.4. Silver nanoparticles antibacterial activity

The effectiveness of silver nanoparticle for antibacterial test was assessed by testing three samples (S1, S2 and V) as illustrated in Fig. 8(a,b). Samples S1 and S2 have inhibition zone 09 mm and 18 mm, respectively for *E. coli* (Fig. 8a) and 17 mm and 19 mm, respectively for *Bacillus cereus* (Fig. 8b). There was no inhibition zone around the sample V.

AgNPs inhibit the growth of microbes by either penetrating inside the bacteria, causing damage to the cell or the Ag^{+} released by AgNPs can interact with disulfide or thiol groups of enzymes, and then disrupt metabolic processes [28,29]. From the results, it is clear that both *E. coli* and *Bacillus cereus* growth were inhibited by samples S1 and S2. However, these microorganisms could survive in the presence of the sample V. The effectiveness of the silver nanoparticles thin film for antibacterial activity was confirmed. The synthesised thin film silver nanoparticles are very effective to inhibit the growth of both gram positive and gram negative of bacteria.

2.5. Contact angle measurement

Surface hydrophilicity of membranes plays an important role in water flux. To characterize the hydrophobicity/hydrophilicity of a material surface, the contact angle (CA) as well as the contact angle hysteresis has to be considered [30,31]. The contact angle is the

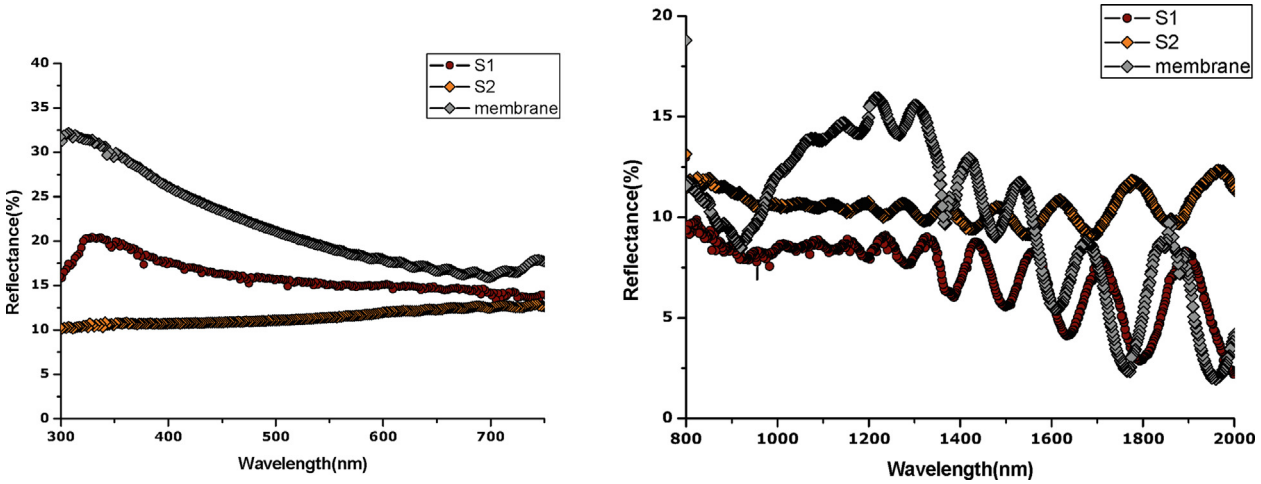

Fig. 4. Specular reflectance of virgin polycarbonate membrane (V) and modified membrane with AgNPs.

Please cite this article as: J. Sackey, A. Fell, J. B. Ngilirabanga et al., Antibacterial effect of silver nanoparticles synthesised on a polycarbonate membrane, Materials Today: Proceedings, https://doi.org/10.1016/j.matpr.2020.04.121

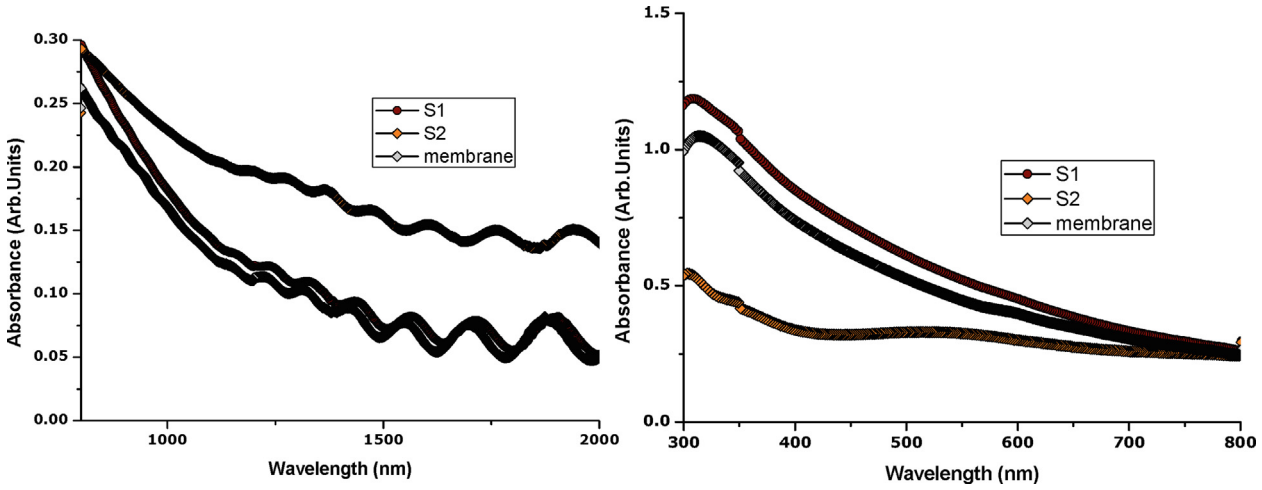

Fig. 5. Absorbance spectra for the virgin membrane (v) and embedded silver nanoparticles (S1 & S2). The virgin membrane (V) and embedded silver nanoparticles membrane via centrifugation (S1) and ultra-sonication (S2) shows surface plasmon resonance between 310 nm.

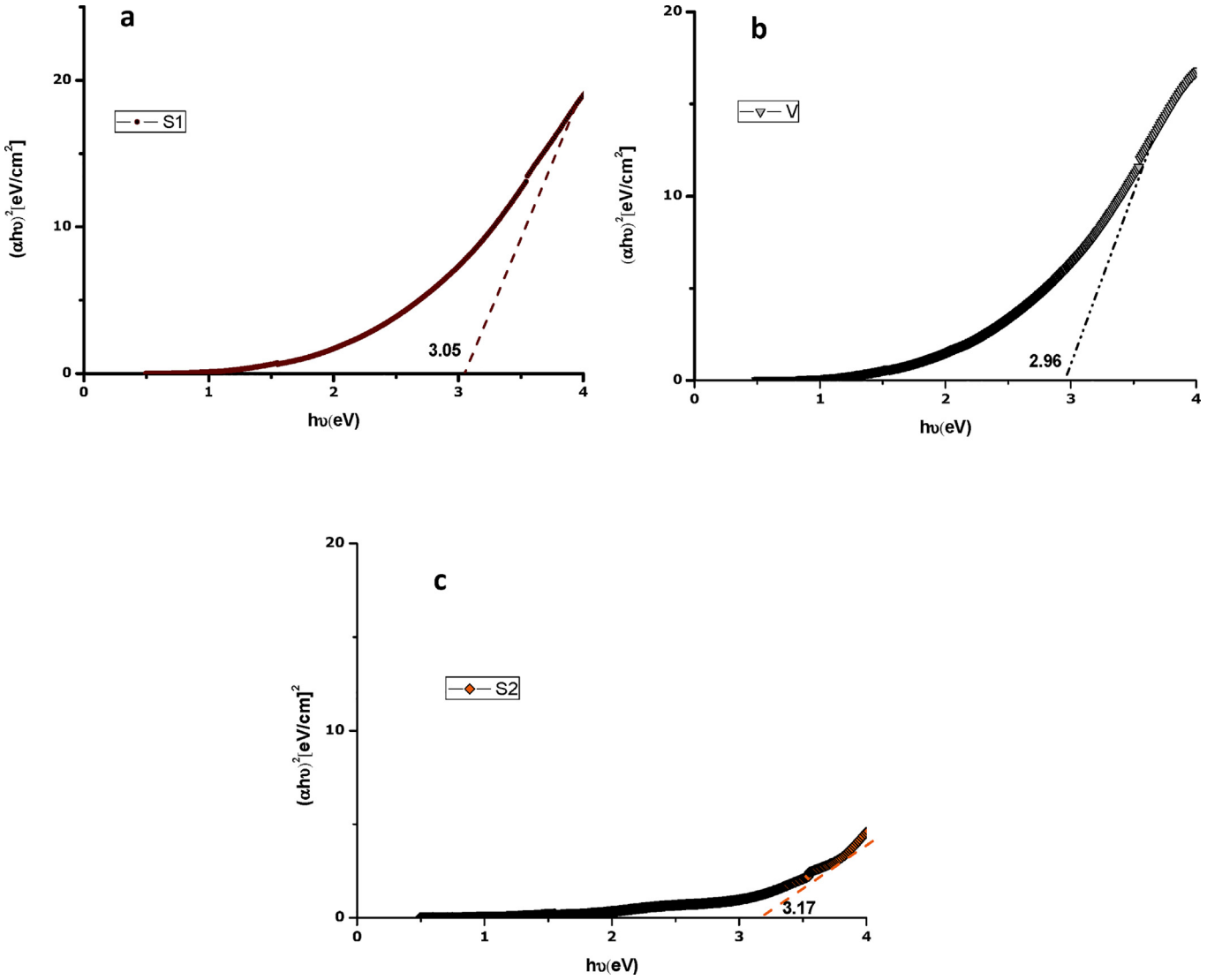

Fig. 6. The energy band gap spectra of the ultra-sonicated AgNPs membrane shows band gap of 3.17.

Please cite this article as: J. Sackey, A. Fell, J. B. Ngilirabanga et al., Antibacterial effect of silver nanoparticles synthesised on a polycarbonate membrane, Materials Today: Proceedings, https://doi.org/10.1016/j.matpr.2020.04.121

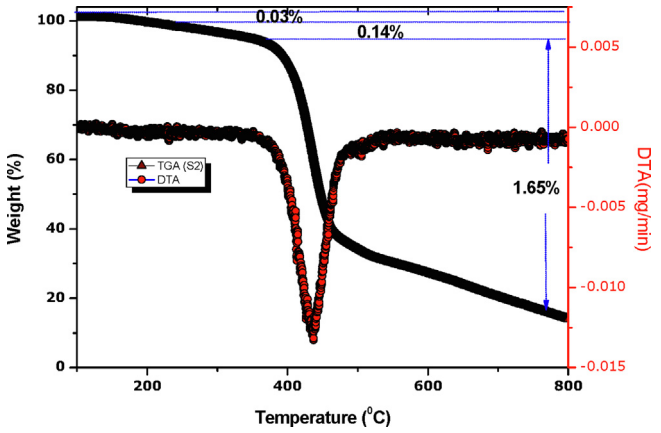

Fig. 7. Thermogravimetric analysis and its derivative form (TGA–DTG curves) on the modified membrane with the silver nanoparticles.

angle at which the liquid/vapor interface meets a given solid. The lower contact angle means the greater tendency for liquid water to wet the membrane and higher hydrophilicity. When liquid water spreads over a surface without the formation of droplets, the surface is said to be hydrophilic. As illustrated in Fig. 9, the values of water contact angles of the three samples (V, S1, S2) are presented. One can clearly observed the virgin membrane (V) has higher contact angle which implies a lesser hydrophilicity. On the contrary, the centrifuged thin film AgNPs membrane (S1) exhibits a lower contact angle and hence a higher wetting ability. It was noted that the hydrophobicity of the membrane decreases after surface modification with the AgNPs. AgNPs have relatively high hydrophobicity as compared to the carboxylic acid groups, present on the membrane which has relatively hydrophilic surface

3. Conclusion

Aqueous extracts obtained from red flowers of *Callistemon viminalis* was used as the reducing agent in green synthesis of AgNPs. The AgNPs were subsequently loaded on a commercialized polycarbonate membrane via ultra-sonication and configuration. The SEM images show nanoparticles of average size of 58.5 nm. The XRD analysis confined a Face-centered cubic silver with lattice parameter a = 4.08620. The synthesised thin film silver nanoparticles are very effective to inhibit the growth of *E. coli and Bacillus cereus.*

CRediT authorship contribution statement

J. Sackey: Methodology, Writing - original draft, Writing - review & editing. **A. Fell:** Writing - review & editing. **J.B. Ngilirabanga:** Methodology, Writing. **L.C. Razanamahandry:** Methodology. **S.K.O. Ntwampe:** Writing - review & editing. **M. Nkosi:** Supervision.

Declaration of Competing Interest

The authors declare that they have no known competing financial interests or personal relationships that could have appeared to influence the work reported in this paper.

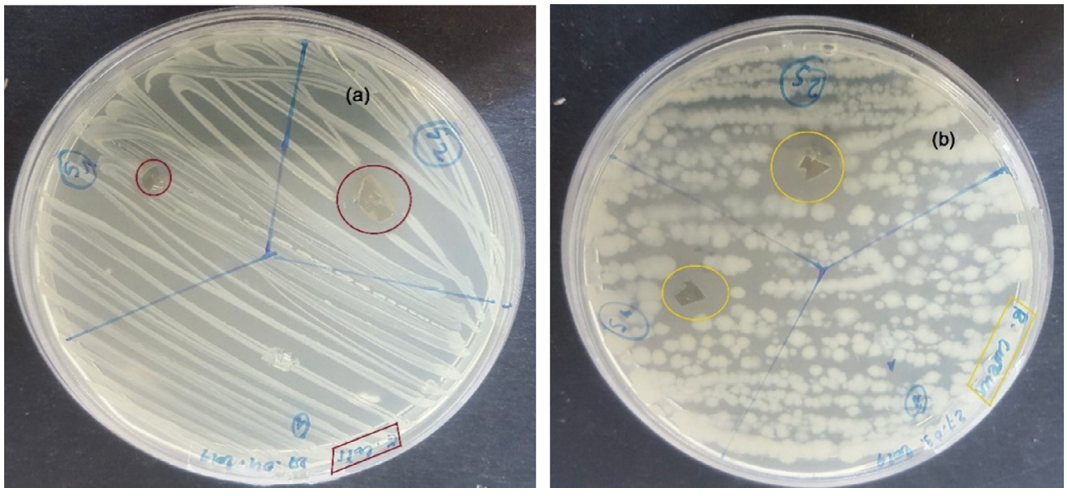

Fig. 8. Antibacterial effectiveness of the silver nanoparticles against (a) Escherichia coli and (b) Bacillus cereus.

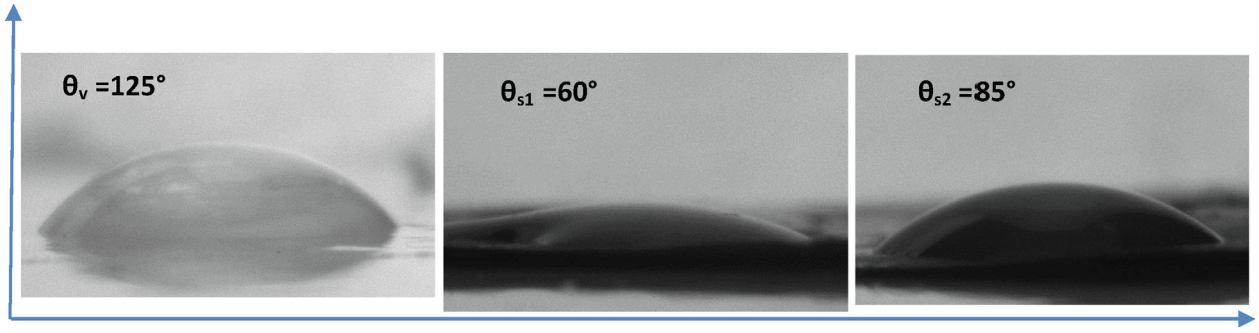

Fig. 9. Water contact angle measurement for (v), (S1), (S2).

Please cite this article as: J. Sackey, A. Fell, J. B. Ngilirabanga et al., Antibacterial effect of silver nanoparticles synthesised on a polycarbonate membrane, Materials Today: Proceedings, https://doi.org/10.1016/j.matpr.2020.04.121

Acknowledgements

This research program was generously supported by grants From the UNESCO-UNISA Africa Chair in Nanosciences& Nanotechnology, National Research Foundation of South Africa (NRF), and iThemba LABS.

References

[1] S.O. Aisida, K. Ugwu, P.A. Akpa, A.C. Nwanya, U. Nwankwo, S.S. Botha, F.I. Ezema, Surfaces and Interfaces 17 (2019) 100359.
[2] S.O. Aisida, K. Ugwu, P.A. Akpa, A.C. Nwanya, P.M. Ejikeme, S. Botha, F.I. Ezema, Materials Chemistry and Physics 237 (2019) 121859.
[3] S.O. Aisida, E. Ugwoke, A. Uwais, C. Iroegbu, S. Botha, I. Ahmad, F.I. Ezema, Journal of Polymer Research 26 (9) (2019) 225.
[4] N.M.I. Alhaji, D. Nathiya, K. Kaviyarasu, M. Meshram, A. Ayeshamariam, Surfaces and Interfaces 17 (2019) 100375.
[5] K. Faulds, W.E. Smith, D. Graham, Analytical Chemistry 76 (2004) 412–417.
[6] B. Thomas, B. Vithiya, T. Prasad, S.B. Mohamed, C.M. Magdalane, K. Kaviyarasu, M. Maaza, Journal of Nanoscience and Nanotechnology 19 (5) (2019) 2640–2648.
[7] A.A. Ezhilarasi, J.J. Vijaya, K. Kaviyarasu, L.J. Kennedy, R.J. Ramalingam, H.A. Al-Lohedan, Journal of Photochemistry and Photobiology B: Biology 180 (2018) 39–50.
[8] C. Ragupathi, R. Azhagu Raj, G. Ramalingam, K. Arun Kumar, N. Mohamed Basith, Advanced Science Engineering and Medicine 8 (11) (2016) 862–867.
[9] M.G. Guzmán, J. Dille, S. Godet, International Journal of Chemical, Molecular, Nuclear, Materials and Metallurgical Engineering 2 (2008) 91–98.
[10] C. Ragupathi, S. Narayanan, M.P. Pachamuthu, N.M. Basith, R. Kannapiran, G. Ramalingam, Advanced Science Engineering and Medicine 10 (9) (2018) 882–886.
[11] M. Huang, L. Du, J.-X. Feng, Science of Advanced Materials 8 (8) (2016) 1641–1647.
[12] G.R. Nasretdinova, R.R. Fazleeva, R.K. Mukhitova, I.R. Nizameev, M.K. Kadirov, A.Y. Ziganshina, V.V. Yanilkin, Russian Journal of Electrochemistry 51 (2015) 1029–1040.
[13] L. Blandón, M.V. Vázquez, D.M. Benjumeab, G. Cirob, Portugaliae Electrochimica Acta 30 (2012) 135–144.
[14] M. Muniz-Miranda, Applied Surface Science 225 (2004) 125–130.
[15] J.J. Laserna, A.D. Campiglia, J.D. Winefordner, Analytica Chimica Acta 208 (1988) 21–30.
[16] J.S. Taurozzi, V.V. Tarabara, Environmental Engineering Science 24 (2007) 122–137.
[17] R.R.A. Hassan, W.S. Mohamed, Applied Physics A 124 (2018) 551.
[18] G. Manimegalai, S. Shanthakumar, C. Sharma, International Nano Letters 4 (2014) 105.
[19] K. Wang, Q. Ma, S.D. Wang, H. Liu, S.Z. Zhang, W. Bao, L.Z. Ling, Applied Physics A 122 (2016) 40.
[20] Y. Zhang, Y. Wan, Y. Shi, G. Pan, H. Yan, J. Xu, Y. Liu, Journal of Polymer Research 23 (2016) 105.
[21] G. Manimegalai, S. Shanthakumar, C. Sharma, International Nano Letters 4 (2014) 1–05.
[22] B.T. Sone, E. Manikandan, A. Gurib-Fakim, M. Maaza, Journal of Alloys and Compounds 650 (2015) 357–362.
[23] J. Sackey, A.C. Nwanya, A.K.H. Bashir, N. Matinise, J.B. Ngilirabanga, A.E. Ameh. . .M. Maaza, Materials Chemistry and Physics 244 (2020) 122714.
[24] V.T. Do, C.Y. Tang, M. Reinhard, J.O. Leckie, Environmental Science & Technology 46 (2012) 852–859.
[25] K. Wang, Q. Ma, S.D. Wang, H. Liu, S.Z. Zhang, W. Bao, L.Z. Ling, Applied Physics A 122 (2016).
[26] G. Mie, Physics (Leipzig) 25 (1976) 377–445.
[27] L. Gharibshahi, E. Saion, E. Gharibshahi, A.H. Shaari, K.A. Matori, Materials 10 (2017) 402.
[28] S. Valsalam, P. Agastian, M.V. Arasu, N.A. Al-Dhabi, A.K.M. Ghilan, K. Kaviyarasu. . .S. Arokiyaraj, Journal of Photochemistry and Photobiology B: Biology 191 (2019) 65–74.
[29] N. Jayaprakash, J.J. Vijaya, K. Kaviyarasu, K. Kombaiah, L.J. Kennedy, R.J. Ramalingam. . .H.A. Al-Lohedan, Journal of Photochemistry and Photobiology B: Biology 169 (2017) 178–185.
[30] J. Sackey, B.T. Sone, K.A. Dompreh, M. Maaza, MRS Advances 3 (2018) 2697–2703.
[31] J. Sackey, Z.Y. Nuru, B.T. Sone, M. Maaza, IET Nanobiotechnology 11 (2016) 71–76.

Please cite this article as: J. Sackey, A. Fell, J. B. Ngilirabanga et al., Antibacterial effect of silver nanoparticles synthesised on a polycarbonate membrane, Materials Today: Proceedings, https://doi.org/10.1016/j.matpr.2020.04.121